The Effecting of a Sudden Step Change on Heat Transfer Coefficient

Dr. Alaa Abbas Mahdi
Asst. Prof.
Eng. College / Kufa Univ.

Hayder Aziz Neema
M. Sc. Mech.Eng.
Eng. College / Kufa Univ.

Bassem Kadhem
M. Sc. Mech.Eng.
Eng. College / Al-Qadessia Univ.

Abstract

Numerical techniques and theoretical results for an incompressible laminar separated flows were presented. For the case of the internal flow over backward facing step. The heat transfer processes and the flow behavior were effected with type of the fluid, expansion ratio, and Reynolds number. It was found that, an increasing in Reynolds number leads to increase the vorticity strength and the size of the recirculation zone in linear relation. This increasing in each of size of the recirculation zone and vorticity strength depends on the expansion ratio. Also, it was found that the average Stanton number in the recirculation zone decreases with increasing of Reynolds number at lower expansion ratios. For high expansion ratios, the average of Stanton number in the recirculation zone, increases with increasing Reynolds number for range of Reynolds number of (Re < 175), and decreasing with increasing Reynolds number for range of Reynolds number of (Re > 175). The results were represented for the reattachment length (Rl) and for the average Stanton number in recirculation zone ($\overline{St}$). Also, velocity distribution, vorticity distributions, temperature distributions, were presented for range of Reynolds number greater than 25 and less than 1000 for different conditions.

Nomenclatures

Symbol	description	unit
S	Size of the step.	m
Rl	Reattachment length.	m
X	Longitudinal coordinate referenced to step position.	m
Y	Transverse coordinate.	m
		m
U	Velocity component in x-direction.	m/s
V	Velocity component in y-direction.	m/s
		m/s
Q	Total velocity.	m/s
P	Pressure.	N/m^2
T	Temperature.	k
Pr	Prandtl number = $c_p \cdot \mu / k$	-
Re	Reynolds number, $\left(\rho \cdot U_{in} \left(AF\right)/\mu\right)$	-
St	Stanton number, $\left(h/\rho \cdot c_p \cdot U\right) = \left(Nu/Re \cdot Pr\right)$	-
Nu	Nusselt number, $\left(h_s/k\right)$	-
Pe	Peclet number=Re . Pr	-
Dx	Distance between left and right sides of control volume.	m
Dy	Distance between upper and lower sides of control volume.	W/K
K	Thermal convection conductance.	J/kg.K
Cp	Specific heat at constant pressure.	J/m^2
Q	Quantity of heat transfer per unit area.	W/m^2K
H	Local heat transfer coefficient.	
R	Ratio between downstream area to upstream area.	-

Greek symbols

symbol	description	unit
α	Thermal diffusivity = $k/\rho \cdot C$	m^2/s
μ	Dynamic viscosity.	kg/m.s
ν	Kinematics viscosity = μ/ρ	m^2/s
ρ	Mass density of fluid.	kg/m^3
τ	Stress.	N/m^2
δ	Displacement boundary layer thickness.	m
ψ	Stream function.	m^2/s
ω	Vorticity.	1/s
δ_x	Distance between left and right sides of control volume.	m
δ_y	Distance between upper and lower sides of control volume.	m

Subscripts

symbol	description
s	At the step position.
F.P	Flat plate condition.
i	Mesh index corresponding to longitudinal direction.
j	Mesh index corresponding to transverse direction.
e	Eastern control volume direction.
w	Western control volume direction.
n	North control volume direction.
s	South control volume direction.
p	Center of control volume.
*	Dimensionless value.
-	Average value.
A	Value at point A.
E	Value at point E.
F	Value at point F.

1- Introduction

In many flows of practical interest, separation of boundary layer and subsequent of the separated layer to a solid surface is unavoidable, such flows occurs in nuclear reactor, gas turbines, combustion chambers, heat exchangers, and cooling systems for equipments [1]. The reattachment flows can pose a serious problem for the heat transfer engineering, because they can cause a large variations

of the local heat transfer coefficient as well as substantial heat transfer augmentation. Convective heat transfer in the separation and reattachment regions following abrupt area changes in tubes and ducts is of considerable technical interest .Therefore, it was needed to study the overall heat transfer coefficient under the effect of separation. The present work study the fluid dynamics and heat transfer characteristics in the separated regions, and the region area of reattachment for laminar flows in rectangular cross-sectional ducts with abrupt increases in flow cross-sectional area. The Navier-Stokes equations and energy conservation equations, which were considered to describe the fluid motion and heat transfer of interest, are nonlinear, because of this non linearity, some difficulties have arisen in numerical as well as in analytical studies. One of the greatest difficulties with the numerical studies is the problem of divergence of the iterative methods. Since an analytical solution of the actual problem is extremely difficult if not possible, a number of assumptions together using the computational fluid dynamic techniques to obtain approximate results. The present work deals with internal flow represented by laminar incompressible flows through a flat duct having backward facing step , as shown in Fig. (1). Attention was focused to study the flow behaviors and mechanism of heat transferred by forced convection in recirculation zones.

The phenomena of flow separation caused by sudden changes in geometries was well known. The importance of such flows to engineering equipment has been stressed in many publications, and attempts have been made to develop advanced experimental and theoretical techniques in order to study carefully flows with separation regions. Though a number of investigations on the flow field have been reported, there appears to be very little published studies concerning the corresponding heat transfer problem in separated region were used the techniques of computational fluid dynamics.

Aung [2] presented heat transfer measurements for laminar flow past backsteps in low speed wind tunnel with expansion ratio of (r=12.5:1) and test section of 20 cm height, 15 cm width, and 61 cm length, step heights of 1.27 cm, 0.64 cm, and 0.38 cm and 1.02 cm, respectively. The results were given for the local heat transfer as well as the average value in separated regions. It was found that the average Stanton number exhibits a minus one half power dependency on the Reynolds number, the local heat transfer increases monotonically across the reattachment point and quantitatively less than flat-plate value. Average Stanton number (for upstream and downstream of backstep) was correlated in the following equation:

$$\overline{St} = 0.787(Re)^{-0.55}\left[\frac{s}{x_s}\right]^{0.72} \qquad ----------(1)$$

Durst et al [3] used the flow visualization and laser-anemometry measurements to report the flow downstream of a plane 3:1 symmetric expansion in a duct with an aspect ratio of 9.2:1 downstream of expansion. Ede et al [4] studied the effect of an abrupt disturbance (0.5 diameter ratio) on water flowing in a pipe. The effect of the abrupt convergence on the local heat transfer coefficient was determined for Reynolds number ranging from 800 to 100,000 in the smallest pipe.

Sinha et al [5] studied the flow over backsteps in laminar range. The results were reported experimentally at a wind speed of 1.8 m/s over three backward facing steps 0.625, 1.25, and 2.5 cm high, the separating boundary layer in all cases was 1.4 cm thick. They found that the dimensionless reattachment length (x_r/s) increases linearly with Reynolds number (Re_s) as long as the reattachment was laminar. Krall and Sparrow [6] was studied experimentally the effect of the flow separation on the heat transfer characteristics in turbulent pipe flow. The flow separation was induced by an orifice situated at the inlet of an electrically heated circular tube. Water was the working fluid and the flow was fully developed. Seki et al [7] studied experimentally heat transfer in the separated reattached and redevelopment region behind a double step in a flat duct, with air as the working fluid. They presented experimental data for the local heat transfer coefficient for fluid flows into the abrupt symmetrical enlargement.

Goldstein et al [8] made experiments on the shear layer following a downstream facing step. Results were reported over a range of 0.36-1.02 cm in step height, 0.61-2.44 m/s in free stream velocity at the step, and 0.16-0.51 cm in boundary layer displacement thickness at the step. They found that the laminar reattachment length was not constant number of step heights as for turbulent flow, but varies with Reynolds number and boundary layer thickness at the step, and given by:

$$\frac{x_r}{\delta_s^*} = 0.01325 \mathrm{Re}_{\delta^*} \left[\left(\frac{s}{\delta_s^*} \right) + 2 \frac{s}{\delta_s^*} \right] \quad \text{----------(2)}$$

Filletti and Kays [9] studied experimentally heat transfer in the separated reattached and redevelopment region behind a double step in a flat duct, with air as the working fluid. Air was blown by a ducted fan into the test section. Sparrow and Kalejs [10] presented experimental investigation for the heat transfer coefficient distributions in the regions of flow separation. Reattachment, and redevelopment along the walls of a channel whose inlet was partially constricted. The experiments were carried out for Reynolds numbers in the laminar range and utilized the naphthalene sublimation technique with air as the working fluid. Seban et al [11] presented the local heat transfer coefficients and recovery factors for separated and reattached turbulent flows as obtained downstream of a flat surface in two dimensional subsonic air flow. Wind tunnel test were made on a rounded nose model with a sudden step down to a flat surface. Najdat [12] used the numerical techniques to analysis a two-dimensional, incompressible, laminar flows in the entrance region of a channel with and without contractions. This constructions representing by forward facing step, backward facing step, or finite step. Finite difference method was used to solve the governing equations which were formulated in stream function-vorticity approach. Nallassamy [13] studied a steady state, two-dimensional, viscous, incompressible flows over a thin obstruction in a channel through the numerical solution of the Navier-Stokes equations using finite difference method. The characteristics of the separated flow behind the obstruction where obtained up to Reynolds number of 1500.

Mei [14] used finite difference method to investigate two-dimensional, laminar, and incompressible fluid flows through a channel with symmetrical and asymmetrical sudden constructions formed by a semi-infinite step change in width

and through cascade. The Navier-Stokes equations in stream function-vorticity form in body fitted coordinates were solved for up to critical Reynolds numbers. Morrision and Napolitano [15] provide a simple efficient and robust numerical technique for solving two dimensional incompressible steady viscose flows at moderate to high Reynolds number using the streamfunction vorticity formulation simultaneously on steeped channel using finite difference method. Roland [16] used the Newton iteration and finite difference method to solve the ensuing algebraic system resulting from discretizing Navier-Stokes equation. In order to avoid high-frequency errors, locally fine grid was used near corner by transformation of the independent variables. As compared with the previous works the present work characterized by the following:

***i*- The present work afforded a theoretical study for knowledge of the effect of affection factors on flow and heat transfer characteristic in wide field by the use of computational fluid dynamics techniques, and this was a complement for Aung's work [2].**

***ii*- The present work adopting stream function vorticity approach [17], like the problems of the present work, after some modifications such as using of converging factors, and non uniform mesh distribution.**

***iii*- The present work afforded a computer program have unlimited capacity in the range of laminar flow.**

2- Theoretical background

The fundamental conservation laws of mass, energy and momentum provide the differential equations; then auxiliary relations, for the thermodynamic, transport properties, and for the boundary conditions, make the mathematical problem complete; and all that was needed to solve the equations, and to deduce from their solution the practically interesting information. The present method of solution was a finite difference one: it confines attention to a finite number of points, distributed irregularly through the flow field as the nodes of the grid; it is primarily for these nodes that will calculate the values of temperature, concentration, and other variables; and, if values are required at intermediate points, it can be obtained by interpolation. Confinement of attention to a two-dimensional array of points entails that the differential equations should be replaced by algebraic ones, relating together the values of the variables which prevail at neighboring nodes. The exist various ways of deriving these "finite difference equations" from the differential ones; the present method employs one which, if not novel, was certainly not conventional. Since was a suitable reason for this practice, which will be explained later; elsewhere, when the conventional procedures bring problems, they have been adopted. Iterative procedures for solving equations were susceptible to a crippling diseases; this was "divergence", i.e. the failure of the method, no matter for how long it was allowed to proceed, to find for the variables a set values which satisfies the equations within the specified limits. Its opposite, "convergence", was the steady progress from the set of values which was supplied at the beginning as "initial guesses", towards a new set which satisfies the equations as closely as is desired. Several of the novelties of the present method have been introduced in order to procure this convergence, for all the circumstances which were of practical interest [17].

2-1 Conservation equations of mass, momentum, and energy for two dimensional laminar flow

To drive the conservation of mass or continuity equation, consider a control volume as shown in Fig. (2) with assumption of steady-state conditions prevail, and neglecting the gradients in z-direction (perpendicular to the plane of the sketch), and the fluid is incompressible. Then the rates of mass flow inlet and outlet the control volume , in x-direction are (ρudy) and $\rho\left[u+\frac{\partial u}{\partial x}dx\right]dy$ **respectively. Thus the net mass flow into the element in x-direction was** $-\rho\frac{\partial u}{\partial x}dxdy$ **. Similarly, the net mass flow into the control volume in y-direction was** $-\rho\frac{\partial u}{\partial y}dydx$ **. Since the net mass flow rate out the control volume must be zero for study flow condition, then:**

$$-\rho\left(\frac{\partial u}{\partial x}+\frac{\partial v}{\partial y}\right)dxdy=0. \quad ----------(3)$$

As in reference [17], the two-dimensional incompressible, steady flow, conservation of mass becomes:

$$\frac{\partial u}{\partial x}+\frac{\partial v}{\partial y}=0 \quad ----------(4)$$

The conservation of momentum equation was obtained from application of Newton's second law of motion to the element. The rates of momentum flow in the x-direction for the fluid flowing across the left- and right-hand vertical faces is shown in Fig.(2) were ($\rho u^2 dy$**)and** $\rho\left[u+\left(\partial u/\partial x\right)dx\right]^2 dy$ **respectively. It should be noted, however, that flow across the horizontal faces will also contribute to the momentum balance in the x-direction. The x-momentum flow entering through the bottom face is** $\rho uvdx$**, and the momentum flow per unit width leaving through the upper face was** $\rho\left(v+\frac{\partial v}{\partial y}dy\right)\left(u+\frac{\partial u}{\partial y}dy\right)dx$ **. The viscous shear force at the bottom face was** $-\mu\left(\frac{\partial v}{\partial x}+\frac{\partial u}{\partial y}\right)dx$ **and at the top face was** $\left[\mu\left(\frac{\partial v}{\partial x}+\frac{\partial u}{\partial y}\right)+\mu\frac{\partial}{\partial y}\left(\frac{\partial v}{\partial x}+\frac{\partial u}{\partial y}\right)dy\right]dx$ **. Thus the net viscous shear in the x-direction was** $\mu\frac{\partial}{\partial y}\left(\frac{\partial v}{\partial x}+\frac{\partial u}{\partial y}\right)dxdy$ **.The normal force on the left face was** $-2\mu\frac{\partial u}{\partial x}dy$ **and on the right face was** $\left(2\mu\frac{\partial u}{\partial x}+2\mu\frac{\partial}{\partial x}\left(\frac{\partial u}{\partial x}\right)dx\right)dy$ **. Thus the net normal force in the direction of motion was** $2\mu\frac{\partial^2 u}{\partial x^2}dxdy$ **. The pressure force on the left face was (pdy) and on the right face was** $-\left[p+\left(\frac{\partial p}{\partial x}\right)dx\right]dy$ **. Thus**

the net pressure force in the direction of motion was $-\left(\frac{\partial p}{\partial x}\right)dxdy$ **. Equating the sum of the forces to the momentum flow rate out of the control volume in the x-direction gives :**

$$\rho\left(u+\frac{\partial u}{\partial x}dx\right)dy-\rho u^2dy+\rho\left(v+\frac{\partial v}{\partial y}dy\right)\left(u+\frac{\partial u}{\partial x}dx\right)dx-\rho vudx=$$

$$-\frac{\partial p}{\partial x}dxdy+\mu\frac{\partial}{\partial y}\left(\frac{\partial v}{\partial x}+\frac{\partial u}{\partial y}\right)dxdy+2\mu\frac{\partial^2 u}{\partial x^2}dxdy \quad ----------(5)$$

As in reference [17], by neglecting second-order differentials and using the conservation of mass equation, the conservation of momentum equation in x-direction reduces to:

$$\rho\left(u\frac{\partial u}{\partial x}+v\frac{\partial u}{\partial y}\right)=-\frac{\partial p}{\partial x}+\mu\left(\frac{\partial^2 u}{\partial x^2}+\frac{\partial^2 u}{\partial y^2}\right) \quad ----------(6)$$

Similarly, the momentum equation in y-direction was

$$\rho\left(u\frac{\partial v}{\partial x}+v\frac{\partial v}{\partial y}\right)=-\frac{\partial p}{\partial y}+\mu\left(\frac{\partial^2 v}{\partial x^2}+\frac{\partial^2 v}{\partial y^2}\right) \quad ----------(7)$$

Fig.(3) shows the rate at which energy was conducted and convected into and out of the control volume. An energy balance requires that the rate of conduction and convection be zero. This yields :

$$k dxdy\left(\frac{\partial^2 T}{\partial x^2}+\frac{\partial^2 T}{\partial y^2}\right)-\left[\rho c_p\left(u\frac{\partial T}{\partial x}+\frac{\partial u}{\partial x}T+\frac{\partial u}{\partial x}\frac{\partial T}{\partial x}dx\right)\right]dxdy-$$

$$\left[\rho c_p\left(v\frac{\partial T}{\partial y}+\frac{\partial v}{\partial y}T+\frac{\partial v}{\partial y}\frac{\partial T}{\partial y}dy\right)\right]dxdy=0 \quad ----------(8)$$

As in reference [18], by using the conservation of mass equation and neglecting second-order terms gives the following expression for the energy equation without dissipation:

$$u\frac{\partial T}{\partial x}+v\frac{\partial T}{\partial y}=\alpha\left(\frac{\partial^2 T}{\partial x^2}+\frac{\partial^2 T}{\partial y^2}\right) \quad ----------(9)$$

The dimensionless stream wise and normal velocity components u^* & v^* were referred to the maximum stream velocity U_{in} , the stream wise and normal dimensionless coordinates (x ,y) are normalized with size of back step (s). The dimensionless Navier-Stokes equations were:

Momentum equation in x-direction

$$u^*\frac{\partial u^*}{\partial x^*}+v^*\frac{\partial u^*}{\partial y^*}=-\frac{\partial p^*}{\partial x^*}+\frac{1}{Re}\left(\frac{\partial^2 u^*}{\partial x^{*2}}+\frac{\partial^2 u^*}{\partial y^{*2}}\right) \quad ----------(10)$$

Momentum equation in y-direction

$$u^*\frac{\partial v^*}{\partial x^*}+v^*\frac{\partial v^*}{\partial y^*}=-\frac{\partial p^*}{\partial y^*}+\frac{1}{Re}\left(\frac{\partial^2 v^*}{\partial x^{*2}}+\frac{\partial^2 v^*}{\partial y^{*2}}\right) \quad ----------(11)$$

Where the Renold number based on the size of back step (s), and the maximum stream velocity U_∞ was represented by:

$$\mathrm{Re} = \frac{\rho U_{in}(AF)}{\mu} \quad ----------(12)$$

As in reference [19],the continuity equation becomes:

$$\frac{\partial u^*}{\partial x^*} + \frac{\partial v^*}{\partial y^*} = 0 \quad ----------(13)$$

As in reference [19], the dimensionless stream function $\psi^*(x^*,y^*)$ is introduced in usual manner:

$$u^* = \frac{\partial \psi^*}{\partial y^*} \quad ----------(14)$$

$$v^* = -\frac{\partial \psi^*}{\partial x^*} \quad ----------(15)$$

It is evident from Eqs. (14) and (15) that the stream function satisfies the continuity equation identically [19]. For this plan flow field, the only non-zero component of vorticity is:

$$\omega^* = \frac{\partial v^*}{\partial x^*} - \frac{\partial u^*}{\partial y^*} \quad ----------(16)$$

Combining the definition of vorticity and velocity components terms of stream function, and cross-differentiating the Navier-Stockes equations to reduce the number of equations and eliminate the pressure terms, a new set of equations was obtained with independent variable (ψ^*) and (ω^*) as following:

$$\frac{\partial^2 \psi^*}{\partial x^{*2}} + \frac{\partial^2 \psi^*}{\partial y^{*2}} = -\omega^* \quad ----------(17)$$

$$\frac{1}{\mathrm{Re}} \frac{\partial^2 \omega^*}{\partial x^{*2}} + \frac{\partial^2 \omega^*}{\partial y^{*2}} = \left(\frac{\partial \psi^*}{\partial y^*} \frac{\partial \omega^*}{\partial x^*} - \frac{\partial \psi^*}{\partial x^*} \frac{\partial \omega^*}{\partial y^*} \right) \quad ----------(18)$$

The numerical technique selected treats the equations such that the stream function derivatives in Eq. (18) are known: hence this equation will be considered to be elliptic in vorticity ω. These two equations are to be solved in a given region subjected to the condition that the value of stream function and the vorticity, or their derivatives, are prescribed on the boundary of the domain.

If the temperature of fluid at inlet (T) and the temperature of the wall surface (T_w), the dimensionless of temperature (T^*) can be obtained from:

$$T^* = \frac{T - T_\infty}{T_w - T_\infty} \quad ----------(19)$$

As in reference [18], the dimensionless energy conservation equations are:

$$u^* \frac{\partial T^*}{\partial x^*} + v^* \frac{\partial T^*}{\partial y^*} = Pr\left(\frac{\partial^2 T^*}{\partial x^{*2}} + \frac{\partial^2 T^*}{\partial y^{*2}} \right) \quad ----------(20)$$

$$\frac{\partial \psi}{\partial y}\frac{\partial T}{\partial x} - \frac{\partial \psi}{\partial x}\frac{\partial T}{\partial y} = Pr\left(\frac{\partial^2 T^*}{\partial x^{*2}} + \frac{\partial^2 T^*}{\partial y^{*2}} \right) \quad ----------(21)$$

Derivation of the finite-difference analogue of the differential equation

There are two ways for deriving finite difference equations from differential ones: Either using Taylor-series expansions, and by integration over control volume, together with assumptions about the distributions of the variables between the nodes of the grid [21]. In the present work the second method was used for two reasons: firstly, it enables the present work to ensure that the conservation laws were obeyed over arbitrarily large oe small portions of the field, a merit which was not possessed by certain of the other schemes which have encountered. Secondly, this procedure lends itself better to physical interpolation, and hence simple in understanding.

Domain of the integration

Fig.(5) displays a part of such a grid; there is shown a typical node (P), and the four surrounding nodes (N, S, E, and W). The finite difference equation will eventually be expressed primarily in terms of the values of the variable at these nodes. The integration of the differential equation will be performed over the area enclosed by the small rectangle, shown by the dotted lines, which encloses the point (P). The sides of this rectangle are supposed to lie midway between the neighboring grid lines. Similar rectangle also exist for other point in the field [21].

Integration of the equations

The result of integration of Eq. (17) is:

$$a_p \psi_p^* = a_e \psi_e^* + a_w \psi_w^* + a_n \psi_n^* + a_s \psi_s^* + b \quad ----------(22)$$

Where:

$$\begin{bmatrix} a_p = a_e + a_w + a_n + a_s & a_e = \dfrac{\left(\delta y_n^* + \delta y_s^*\right)}{\delta x_e^*} & a_w = \dfrac{\left(\delta y_n^* + \delta y_s^*\right)}{\delta x_w^*} \\ b = \omega_p^* \left(\delta x_e^* + \delta x_w^*\right)\left(\delta y_n^* + \delta y_s^*\right) & a_n = \dfrac{\left(\delta x_e^* + \delta x_w^*\right)}{\delta y_n^*} & a_s = \dfrac{\left(\delta x_e^* + \delta x_w^*\right)}{\delta y_{sn}^*} \end{bmatrix}$$

Energy conservation equation is:

$$\frac{\partial\left(u^* T^*\right)}{\partial x^*} + \frac{\partial\left(v^* T^*\right)}{\partial y^*} = \frac{1}{Pe}\left(\frac{\partial^* T^*}{\partial x^{*2}} + \frac{\partial^* T^*}{\partial y^{*2}} \right) \quad ----------(23)$$

The integration of this equation is:

$$a_p T_p^* = a_e T_e^* + a_w T_w^* + a_n T_n^* + a_s T_s^* \quad ----------(24)$$

Where:

$$\left[\begin{array}{ll} a_p = a_e + a_w + a_n + a_s & \\ a_e = \dfrac{1}{Pe}\dfrac{\left(\delta y_n^* + \delta y_s^*\right)}{\delta x_e^*} + \max.\left(0, -u_e^*\left(\delta y_n^* + \delta y_s^*\right)\right) & a_w = \dfrac{1}{Pe}\dfrac{\left(\delta y_n^* + \delta y_s^*\right)}{\delta x_w^*} + \max.\left(0, +u_w^*\left(\delta y_n^* + \delta y_s^*\right)\right) \\ a_n = \dfrac{1}{Pe}\dfrac{\left(\delta x_e^* + \delta y_w^*\right)}{\delta y_n^*} + \max.\left(0, -v_n^*\left(\delta x_e^* + \delta x_w^*\right)\right) & a_s = \dfrac{1}{Pe}\dfrac{\left(\delta x_e^* + \delta x_w^*\right)}{\delta y_s^*} + \max.\left(0, +v_s^*\left(\delta x_e^* + \delta x_w^*\right)\right) \end{array}\right]$$

Tank and tube scheme or upwind scheme

As shown in Fig.(6), the control volumes can be thought to be stirred tanks that are connected in series by short tubes. The flow through the tube represents convection, while the conduction through the tank walls represents diffusion. Since the tanke are stirred each contains a uniform temperature fluid. Then it is appropriate to suppose that the fluid flowing in each connecting tube has temperature that prevails in the tank on the upstream side. Normally the fluid in the tube would not know anything about the tank toward it is heading but would carry the full legacy of the tank from which it has come. This is the essence of the tank and tube scheme or upwind scheme [21].

Conditions for converge

The convergence of an iterative solution of Eqs. (22) or (24) may be procured if the following conditions are satisfied [21]:

i. **The value of ($(a_e+a_{w+}a_n+a_s)$ / a_p) must be less than or equal to unity at every node of the grid.**
ii. **This value must be less than unity on at least one grid node.**
iii. **This value and (b) in Eqs. (22) or (24) must not vary too greatly one cycle of iteration to another.**

Convection heat transfer

Before obtaining the Stanton number and Nusselt and number the convection process must be examined in some detail and relate the convection of heat to the flow of fluid. The first point to note is that the velocity decreases in the directions to word the surface as a result of viscous forces acting in the fluid. Since the velocity of the fluid layer adjacent to the wall is zero , the heat transfer between the surface and this fluid layer by conduction (according to reference [1]) must be:

$$Q = -k\left.\frac{\partial T}{\partial y}\right|_{y=0} = h\left(T_w - T_\infty\right) \quad ----------(25)$$

Although this equation suggests that the process can be viewed as conduction the temperature gradient at the surface $\left(\dfrac{\partial T}{\partial y}\right)_{y=0}$ **is determined by the rate at which the fluid farther from the wall can transport the energy into the mainstream. In convection heat transfer, the unknown parameter is the heat transfer coefficient. From Eq.(24):**

$$-k\left.\frac{\partial T}{\partial y}\right|_{y=0} = h(T_w - T_\infty) \quad ----------(26)$$

Dividing by step size (T_w-T_∞) and multiply with (s), it gives:

$$\frac{hs}{k} = \frac{\left(\frac{\partial T}{\partial(y/s)}\right)}{T_w - T_\infty} \quad ----------(27)$$

Inspection of this equation suggest that the appropriate dimensionless form of the heat transfer coefficient is the so-called Nusselt number (Nu) defined by:

$$Nu = \frac{hs}{k} \quad ---(28)$$

Therefore: $$Nu = \frac{\partial T^*}{\partial y^*} \quad --------(29)$$

Computation procedures

The solution of the governing partial differential Eqs. (17), (19) and (22) was obtained by using a finite difference numerical scheme and to get a stable and converged solution, upwind scheme was used for non uniformly grid distributed. The stream function and vorticity equations are first solved and their results stored. The stored information was then used to obtain the solution of the energy equation. The solution procedure starts by supplying initial guesses of the stream function and vorticity then computes a converged solution by iteration. Convergence of the solution was considered satisfactory when the percentage normalized residuals of each variable (□□□or □□□□□□) between any two successive iterations (Summed over the whole calculation domain) where less than 10^{-6}. The language of technical computing MATLAB was used to build a spatial program to solve these equations. As shown in Fig.(7) where (s) is the step size, (x) horizontal coordinate referenced to the step position, and (y) vertical coordinate. The calculations were started at a distance of (5) times of the step size upstream of back step. Down stream of the back step the grids are extended for a distance of (15) times of the step size.

Boundary conditions

The differential equations Eqs. (17), (19) and (23) have been solved within the limited region shown in Fig.(7), and within the following boundary conditions:

1-On inlet part AF (uniform inlet flow)

a.Stream Function $$\psi^* = y^* - y_F^* \quad ----------(30)$$

b. Vorticity [13] $$\omega^* = 0 \quad --------(31)$$

c. Temperature $$T^* = 0 \quad --------(32)$$

2-On solid boundaries

a.Stream Function

Walls (FE, DC, and ED) $$\psi^* = 0 \quad ------(33)$$

Wall (AB) $$\psi^* = \Psi_A^* \quad -----(34)$$

b. Vorticity [12]

Walls(FE & DC) $$\omega^* = 3\frac{\left(\psi^*_{i,j+1} - \psi^*_{i,j}\right)}{\left(y_{j+1} - y_j\right)^2} - \frac{1}{2}\omega^*_{i,j+1} \quad ------(35)$$

Wall ED $$\omega^* = 3\frac{\left(\psi^*_{i+1,j} - \psi^*_{i,j}\right)}{\left(x_{i+1} - x_i\right)^2} - \frac{1}{2}\omega^*_{i+1,j} \quad ------(36)$$

Wall (AB) $$\omega^* = 3\frac{\left(\psi^*_{i,j} - \psi^*_{i,j-1}\right)}{\left(y_j - y_{j-1}\right)^2} - \frac{1}{2}\omega^*_{i,j-1} \quad ------(37)$$

c. Temperature

At unheated region $T^* = 0 \quad -----(38)$

At heated regions $T^* = 0 \quad -----(39)$

3- BC in a position with long distance from the back step position, all of flow properties in each node were equal to the neighbored properties node in the up stream part [22].

a. Stream Function $\psi^* = \psi^*_w \quad ------(40)$

b. Vorticity $\omega^* = \omega^*_w \quad ------(41)$

c. Temperature $T^* = T^*_e \quad ------(42)$

3- Results and discussions

A discussions were made for the fluid flow inside flat duct with *a* symmetric sudden expansion. The study was performed to investigate the effect of Rynolds number, expansion ratio, and Prandtl number on each of the size of the separated region, wall vorticity, temperature distributions, Nusselt number distribution, and Stanton number distribution. To give a good indication about the influence of effecting factors, results were formulated using modern techniques and presented in detailed using MATLAB and SURFER software.

Size of the separated region

The typical flow patterns obtained from the numerical solution of the flow inside duct with backward facing step were shown in Figs. (8) to (10). The separation starts down stream of the corner and the dividing streamline was originated from a point below the corner and reattached to the wall after traveling a distance called reattachment length. The dividing stream line □□□□□□□started from step to point of attachment where the local wall vorticity equal to zero □□□□□□, but in this case; the reattachment length effected only on Reynolds number for a given step size (s), and expansion ratio (r). The size of the separated region increases with increasing Reynolds number due to increasing the reattachment length. Fig. (11) shows the distribution of the dimensionless axial component of velocity (u / U) for Reynolds number of (Re = 400), and expansion ratio of (r=4:3). Fig. (12) shows the distribution of the dimensionless transverse component of velocity *v* / *U* for Reynolds number of (Re=400), and expansion ratio of (r=4:3). Fig.(13) shows the relation between Reynolds number, and dimensionless of reattachment length for various values of expansion ratios. It can be seen from this figure that the reattachment length increases with increasing Reynolds number for range of Reynolds number □□Re □□250□□, and the reattachment length

increases with increasing expansion ratio. The influencing parameters on reattachment length is correlated by the following equation:

$$\frac{Rl}{s} = 0.2300(Re)^{0.55} \quad ---------(43)$$ **for expansion ratio of (r=4:3)**

$$\frac{Rl}{s} = 0.2614(Re)^{0.55} \quad ---------(44)$$ **for expansion ratio of (r=3:2)**

Vorticities

Figs. (14), to (16) show the contour lines of the dimensionless vorticity distributions for different values of expansion ratios and Reynolds number. It was shown that the heavy concentration of contour lines near the sharp corner indicate a high vorticity gradients in this region as expected. It was seen that the vorticity which was very strong near the corner of the step is swept and transported into the recirculation region. Figs. (17) to (19) show the relation between the lower wall vorticity versus the dimensionless distance down stream of back step (x/s) for different values of Reynolds numbers and expansion ratios. It is noted that the local value of wall vorticity converged to an constant value at distance far away from back step location. These figures also show that the local wall vorticity increases with increasing Reynolds number or decreasing initial dimensionless displacement boundary layer thickness. Figs. (20) to (22) show the relation between the upper wall vorticity versus the distance down stream of inlet position (x/s) for different values of Reynolds numbers. It was shown that the maximum local wall vorticity accrues at fully developed position, and also it was shown that an increasing in Reynolds number leads to increase the local wall vorticity.

Heat transfer coefficient

To compute the Stanton number and Reynolds number as a function of influence parameters. Figs. (23) to (25) demonstrated the dimensionless temperature contours for different values of Reynolds number, and expansion ratios. These figures show that the concentration of temperature contours increases at the walls with increasing Reynolds number. Figs. (26) to (28) show the local Nusselt number distribution downstream of back step for different values of Reynolds, and expansion ratios. Increasing of Reynolds number (or decreasing of expansion ratio) leads to increase the value of local Nusselt number distribution. Figs. (29) to (31) show the local Stanton number distribution downstream of back step for different values of Reynolds, at Prandtl number of $P_r = 0.72$, and expansion ratios. Increasing of Reynolds number (or increasing of expansion ratio) leads to decreases the value of local Stanton number distribution. Fig. (32) shows the average value of Nusselt number versus Reynolds number for three expansion ratios. This figure indicate that the larger expansion ratios leads to decrease the value of average Nusselt number. Fig. (33) shows the average value of Stanton number versus Reynolds number for three expansion ratios at Prandtl number of $P_r=0.72$ .This figure indicate that the larger expansion ratios leads to decreases the value of average Stanton number. The average Stanton number in recirculation zone was correlated by the following equation:

$$\overline{St} = 0.135(Re)^{-0.55} \quad -------(45)$$ **for expansion ratio of (r=1:3)**

$\overline{St} = 0.1242(Re)^{-0.55}$ ––––––– (46) **for expansion ratio of (r=3:2)**

4- Conclusions

The present numerical techniques and solutions for internal fluid flow enable us to examine the effecting of a number of factors which are considered the main controller keys on each of separation, reattachment, redevelopment, and the heat transfer process in the separated regions. The main effecting factors on the size of the separated region are initial shear layer thickness, and Reynolds number. In addition to these factors the Prandtl number, affects the heat transfer processes. From the results it can be concluded that:

1-An increasing in Reynolds number leads to increase the vorticity strength, and the size of the recirculation zone in linear relation. This increasing in each of size of the recirculation zone and vorticity strength depends on the expansion ratio, it was found that the rate of this increasing, increases with increasing expansion ratio. The reattachment length was correlated as a function of Reynolds number and expansion ratio by Eqs. (43) and (44).

2. The average Stanton number in the recirculation zone decreases with increasing of Reynolds number at lower expansion ratios, but for high expansion ratios, the average of Stanton number in the recirculation zone increases with increasing Reynolds number for range of Reynolds number of (Re < 175), and decreasing with increasing Reynolds number for range of (Re > 175). For this case studied the average Stanton number in recirculation zone were correlated by Eqs. (45) and (46).

تأثير التغير التدريجي المفاجئ للمقطع على معامل انتقال الحرارة

المستخلص

تعرض الدراسة الحالية نتائج وتقنيات عددية لتحليل جريان طباقي لا انضغاطي في حالة الانفصال. بالنسبة لحالة الجريان الداخلي فوق الحاجز التدريجي ذو التوجيه الخلفي، فان عملية انتقال الحرارة وطريقة تصرف الجريان تكون متأثرة بعدة عوامل كنوع المائع،نسبة التوسع، و عدد رينولدز. لقد وجد إن أي زيادة في عدد رينولدز تؤدي إلى زيادة في كل من شدة الدوامات وحجم منطقة إعادة التدوير ضمن علاقة خطية. وهذه الزيادة في كل من حجم منطقة إعادة التدوير وشدة الدوامات تعتمد على نسبة التوسع، وقد وجد كذلك إن متوسط عدد ستانتون في منطقة إعادة التدوير يتناقص بزيادة عدد رينولدز عند نسب توسع صغيره. وفي حالة نسب التوسع الكبيرة فان معدل عدد ستانتون يزداد بزيادة عدد رينولدز ضمن مدى معين من عدد رينولدز يتراوح في حدود (Re<175)، وان متوسط عدد ستانتون يتناقص بزيادة عدد رينولدز ضمن مدى معين من عدد رينولدز يتراوح بحدود (Re>175). وقد تم تمثيل بعض النتائج التي تم الحصول عليها لهذه الحالة المدروسة ببعض المعادلات الرياضية والتي تشمل طول اعادة التلامس(Rl) و معدل عدد ستانتون ($\overline{St}$) في منطقة إعادة التدوير. ولقد تم رسم خطوط الانسياب، منحنيات توزيع السرعة، منحنيات توزيع دالة الدوامة، ومنحنيات توزيع درجات الحرارة لمدى واسع من عدد رينولدز يتراوح بين 25 و 1000 وبضروف مختلفة.

References

1. Frank K., and Mark S.; "Principles of Heat Transfer", 5th edition, PWS Publishing Company, 1997
2. Aung W.; "An Experimental Study of Laminar Heat Transfer Downstream of Backsteps", ASME Journal of Heat Transfer, vol. 105, PP. 823-829, 1983
3. Durst F., Melling A., and Whitelaw J.; "Low Reynolds Number Flow over a Plane Symmetric Sudden Expansion", Journal of Fluid Mech., vol. 64, Part 1, PP. 111-128, 1974
4. Ede, A. , Hislop C., and Morris R.; "Effect on the Local Heat Transfer Coefficient in a Pipe of an Abrupt Disturbance of the Fluid Flow; Abrupt Convergence and Divergence of Diameter Ratio 2", Proceedings of the Institution of Mechanical Engineering, London, vol. 170, No. 38, 1956
5. Sinha S. , Gupta A. , and Oberai M.; "Laminar Separating Flow over Backsteps and Cavities" Part I (Backsteps), AIAA Journal, vol. 19, No. 12, PP. 1527-1530, 1981
6. Sparrow, E. , and Krall K.; "Turbulent Heat Transfer in the Separated, Reattached, and Redeveloped Regions of Circular Tube", Journal of Heat Transfer, P. 131, 1966
7. Seki N., Fukusako S., and Hirata T.; "Effect of Stall Length on Heat Transfer in Reattached Region Behind a Double Step at Entrance to an Enlarged Duct", Int. J. Heat and Mass Transfer, vol. 19, PP. 700-702, 1976
8. Goldstein R. , Eriksen V., Olson R. , and Eckert E.; "Laminar Separation, Reattachment, and Transition of the Flow over a Downstream-Facing Step", Transactions of the ASME, Journal of Basic Engineering,
PP. 732-741, 1970
9. Filetti E., and Kays W.; "Heat Transfer in Separated, Reattached, and Redevelopment Regions Behind a Double Step at Entrance to A flat Duct", Transactions of the ASME, Journal of Heat Transfer,
PP. 163-168, 1967
10. Sparrow E. and Kalejs J.; "Local Convective Transfer Coefficient in a Channel Downstream of Partially Constricted Inlet", Int. J. Heat and Mass Transfer, vol. 20, PP. 1241-1249, 1977
11. Seban R. , Emery A., and Levey A.; "Heat Transfer to Separated and Reattached Subsonic Turbulent Flows Obtained Downstream of
a Downstream of a Surface Step", Journal of the Aerospace Sciences, December, 1959
12. Najdat N.; "Laminar Flow Separation in Constructed Channel", Ph. D Thesis, Michigan State University, 1987
13. Nallasmy M.; "Numerical Solution of the Separating Flow due to an Obstruction", Journal of Computer and Fluids, vol. 14, No. 1, PP. 59-68, 1986
14. Mei R.; "Navier-Stokes Solution for Laminar Incompressible flows in Forward-Facing Step Geometries", AIAA Journal, vol. 24, PP. 1106-1111, 1980
15. Morrison J., and Napolitano M.; "Efficient Solutions of Two Dimensional Incompressible Steady Viscous Flows", Journal of Computer and Fluids, vol. 16, No. 2, PP. 119-132, 1988
16. Roland H.; "The Numerical Solution of The Laminar Flow in a Constricted Channel at Moderately High Reynolds Number Using Newton Iteration", Int. J. For Numer. Meth. In Fluids, vol. 11,
PP. 247-258, 1990
17. Anderson J.; "Computational Fluid Dynamics", 1st edition, McGraw-Hill, 1995
18. Holman J. "Heat Transfer ", 5th edition, McGraw-Hill, 1981
19. John A., and Clayton T.; "Engineering Fluid Mechanics", 6th edition, John Wiley and Sons. Ic., New York,1997
20. Petrovic Z., and Stupar S.; "Computation Fluid Dynamics One", Flow", 1st edition, Mechanical Engineering Faculty Belgrade, 1996
21. Patankar V.; "Numerical Heat Transfer and Fluid Flow", 1st edition, McGraw-Hill, Flow", 1st edition, McGraw-Hill, 1980
22. David W., and Frank T.; "Implicit Solution of the unsteady Navier-Stokes Equation for Laminar Flow Through an Orifice within a Pipe" Journal of Computer and Fluids, vol. 2, PP. 295-315, 1974

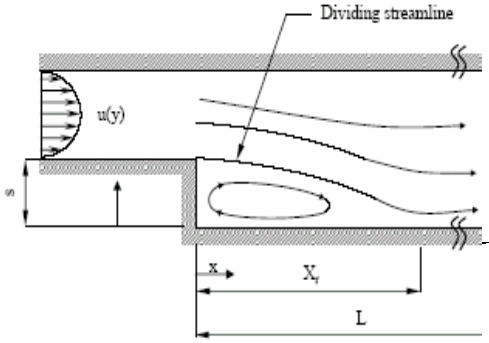

Fig. (1) Internal flow backward facing step

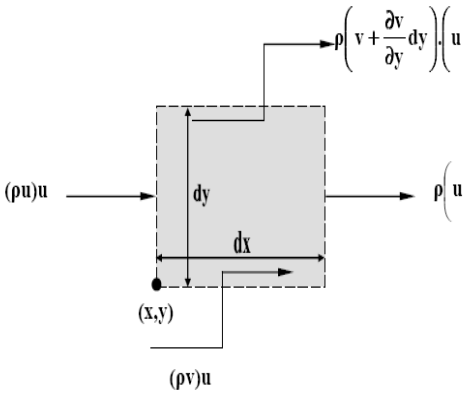

(a) Momentum fluxes

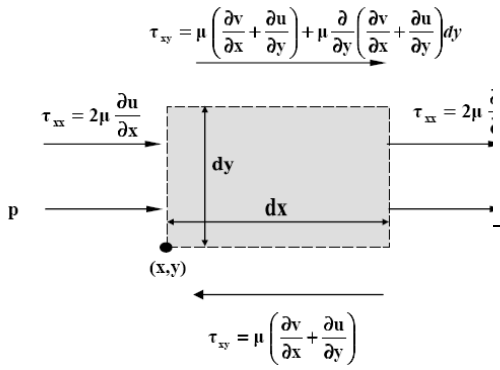

(b) Forces

Fig.(2) Differential control volume for conservation of momentum in a two dimensional incompressible flow

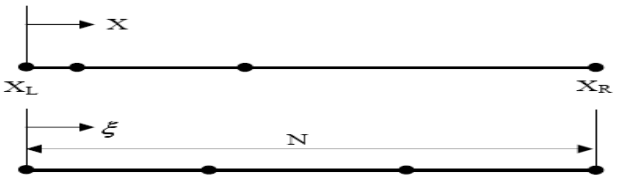

Fig. (4) Symbols for stretching function [20]

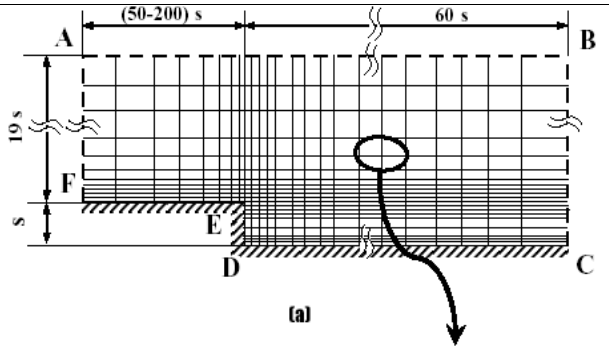

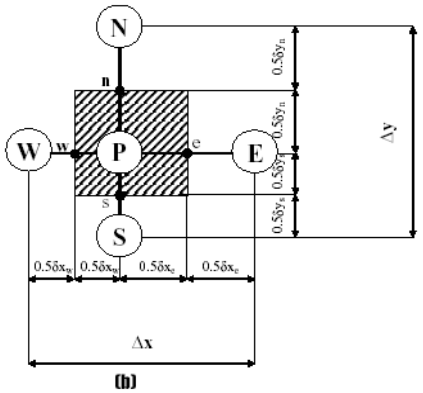

Fig. (5) Typical grid distribution
(a) Grid distribution (b) Control volume

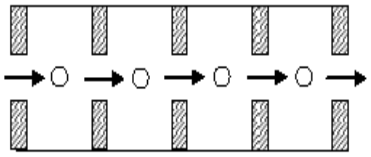

Fig. (6) Tank and tube model [21]

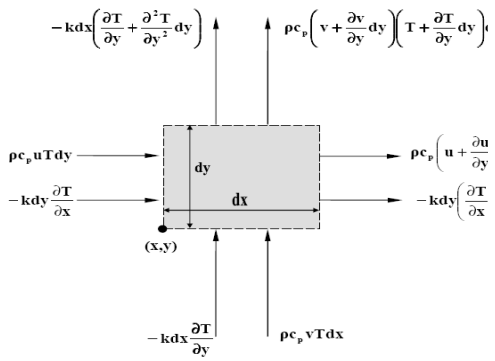

Fig. (3) Differential control volume for conservation of energy in two dimensional incompressible laminar flow

Fig. (7) Typical grid distribution for finite difference solution
[a]: r=4:3 [b]: r=3:2 [c]: r=2:1

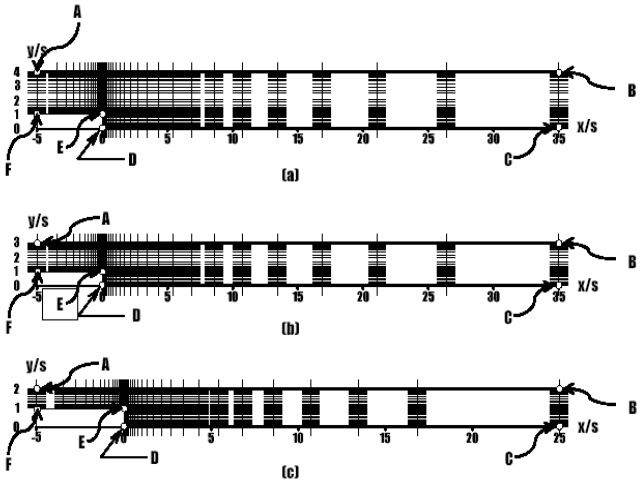

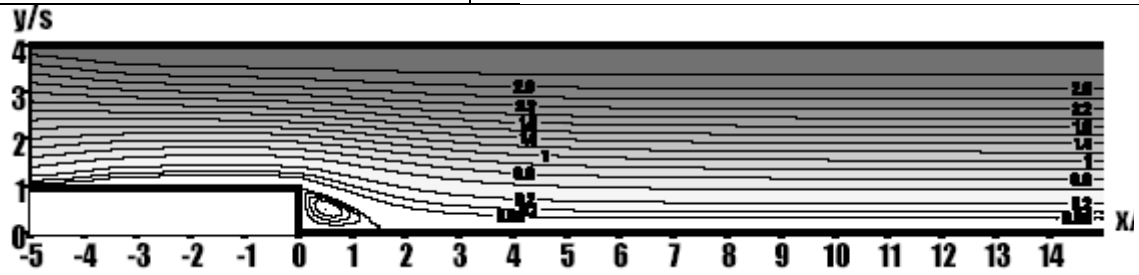

[a]: Re=25

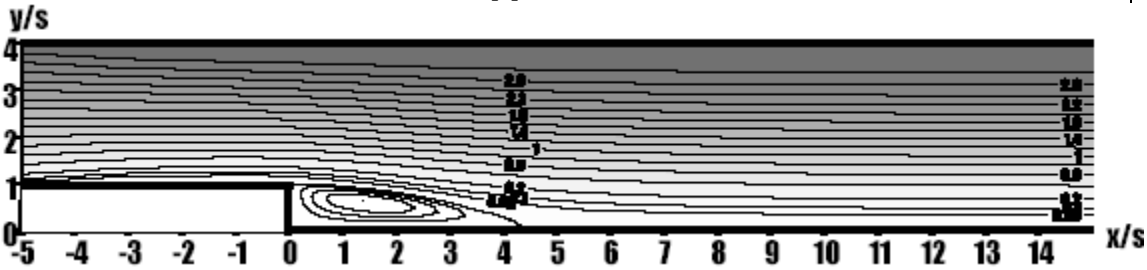

[b]: Re=200

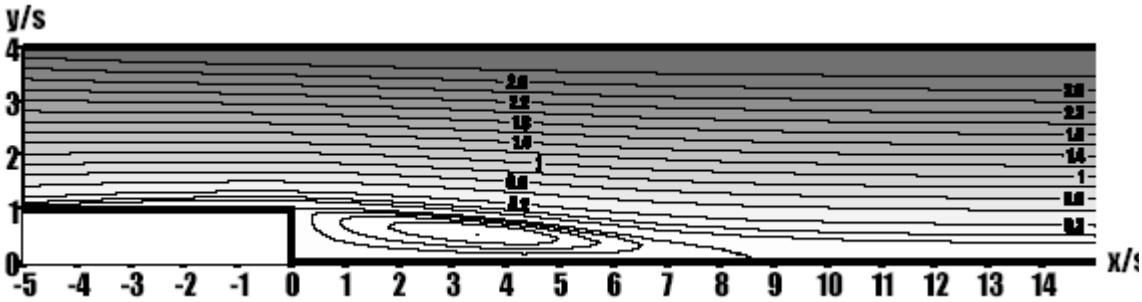

[c]: Re=800

Fig. (8) Stream lines patterns for different values of Reynolds number at r=4:3

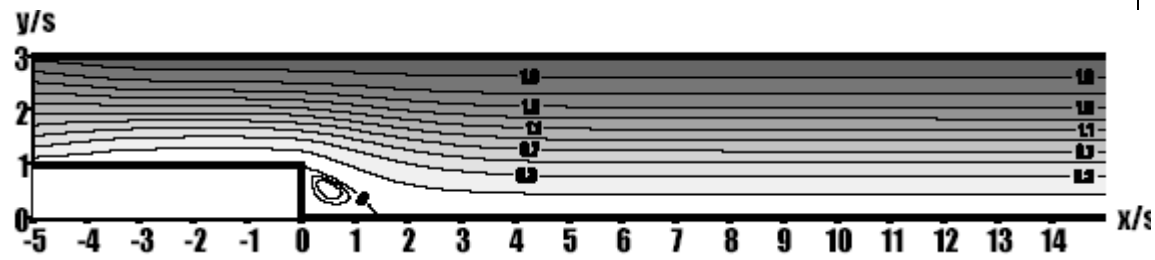

[a]: Re=25

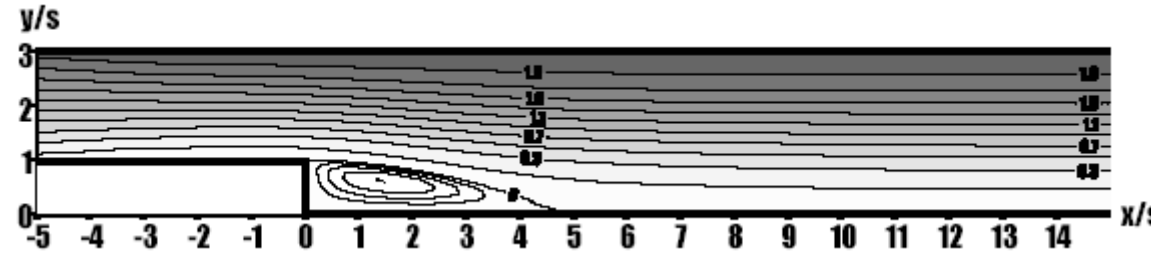

[b]: Re=200

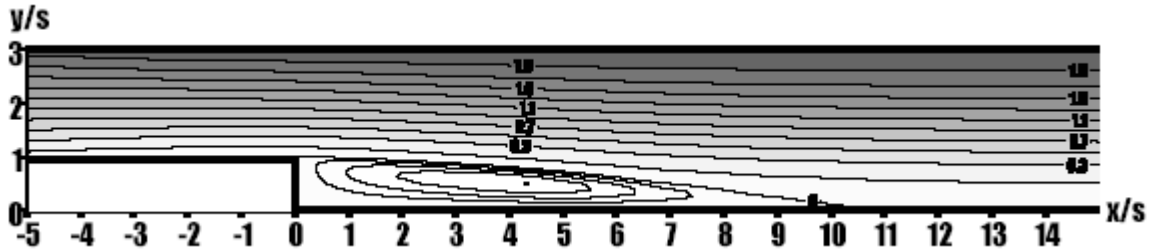

[b]: Re=800

Fig. (9) Stream lines patterns for different values of Reynolds number at r=3:2

[a]: Re=25

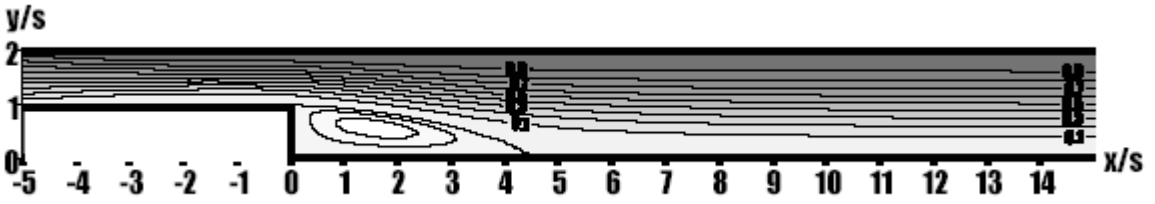

[b]: Re=200

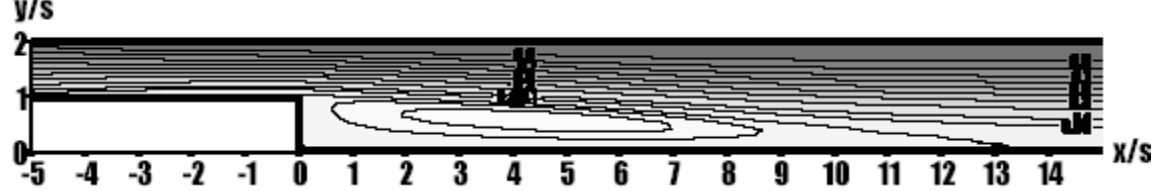

[c]: Re=800

Fig. (10) Stream lines patterns for different values of Reynolds number at r=2:1

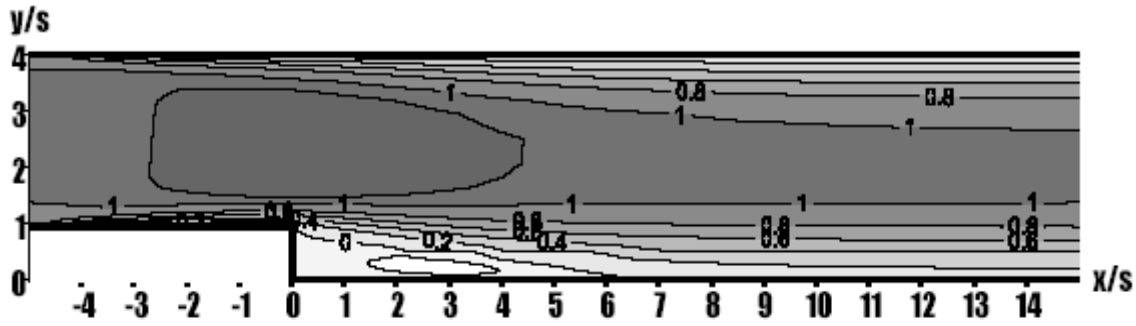

Fig. (11) Dimensionless axial component of velocity contours at Re=400 and r=4:3

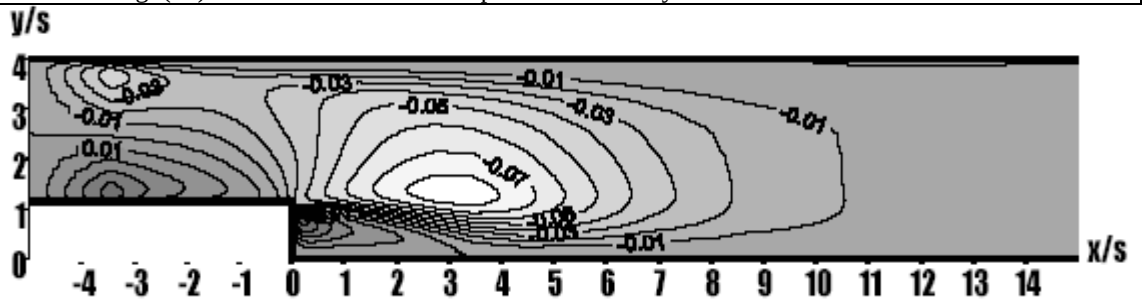

Fig. (12) Dimensionless transverse component of velocity contours at Re=400 and r=4:3

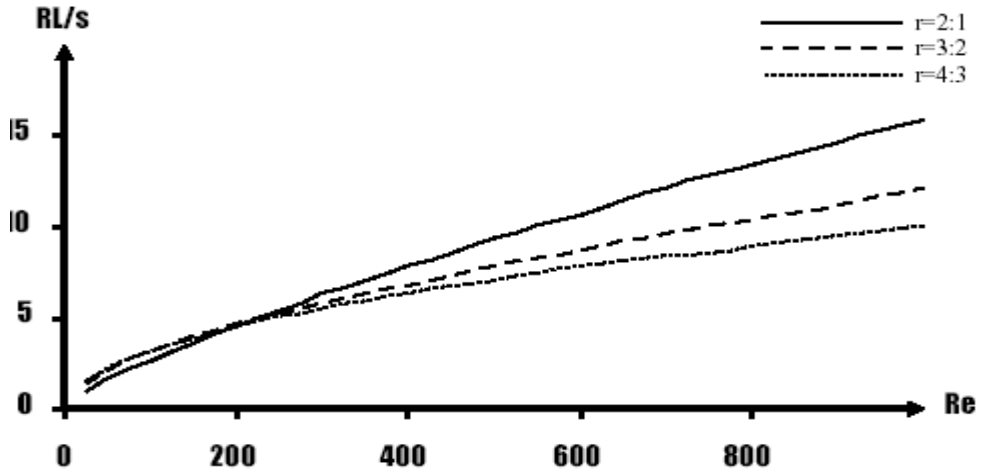

Fig. (13) Dimensionless reattachment length vs. Reynolds number for different of expansion ratio

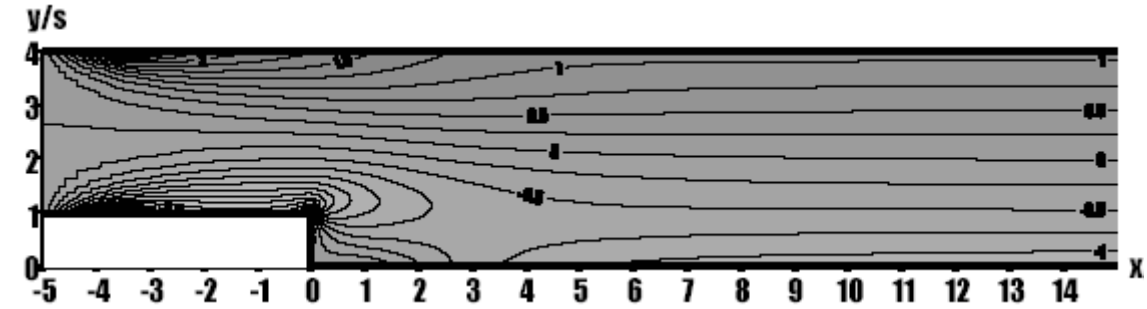

[a]: Re=25

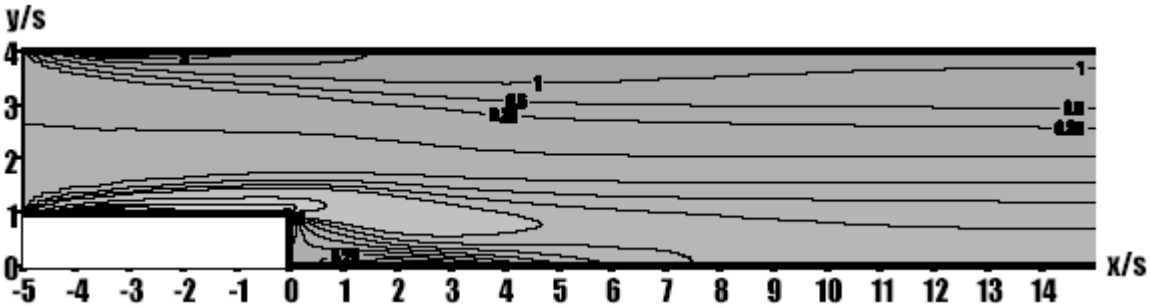

[b]: Re=200

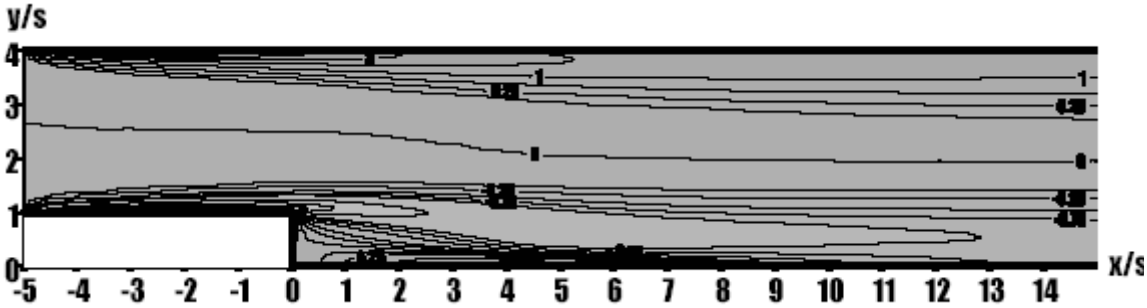

[c]: Re=800

Fig. (14) Vorticity contours for different of Reynolds number at r=4:3

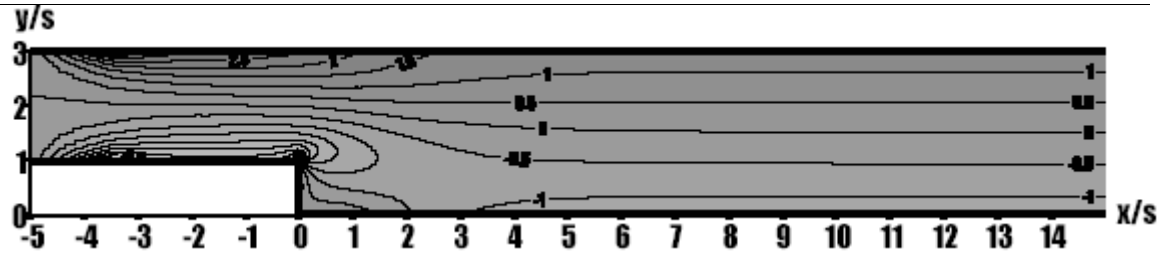

[a]: Re=25

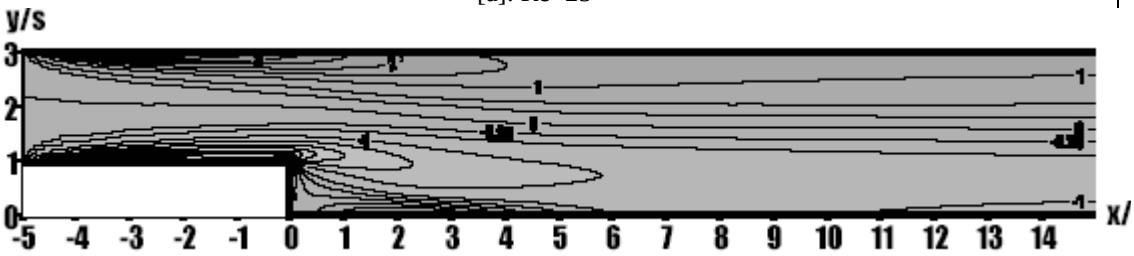

[b]: Re=200

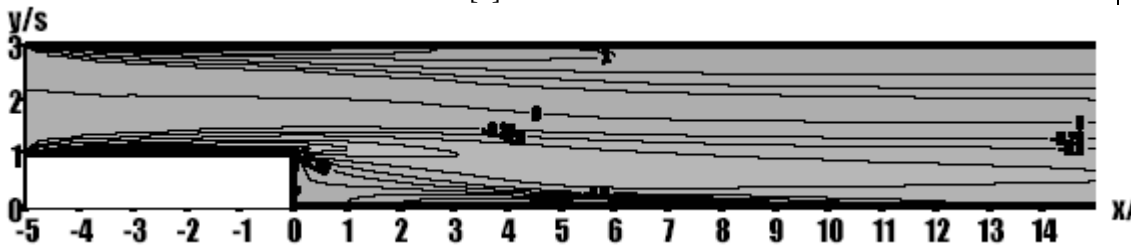

[c]: Re=800

Fig. (15) Vorticity contours for different of Reynolds number at r=3:2

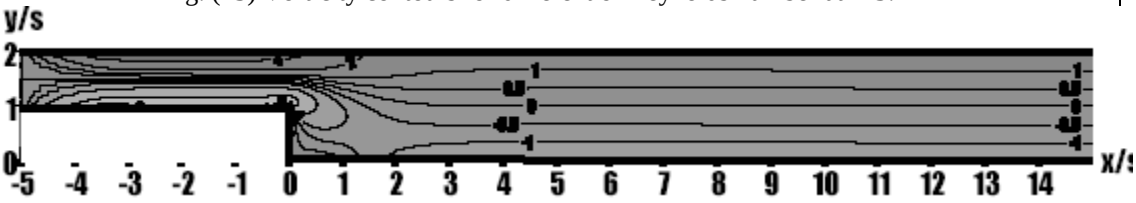

[a]: Re=25

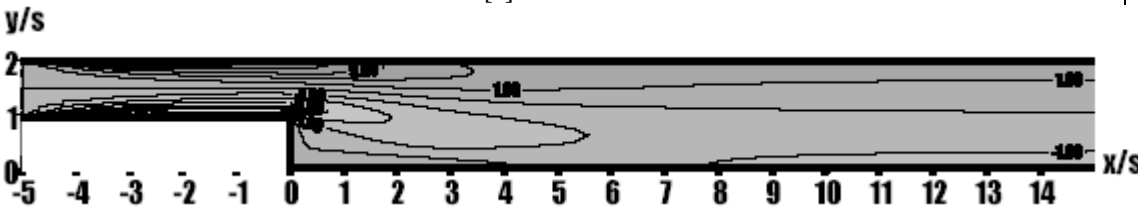

[b]: Re=200

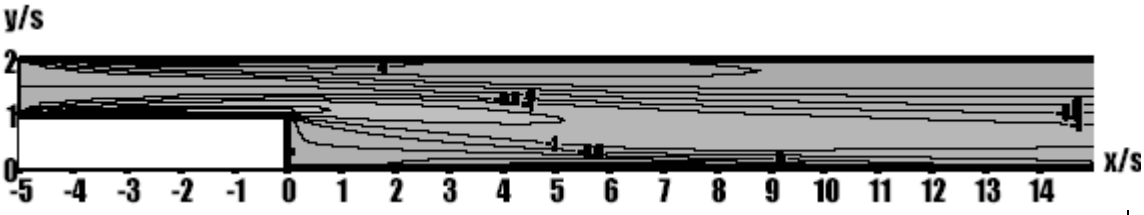

[c]: Re=800

Fig. (16) Vorticity contours for different of Reynolds number at r=2:1

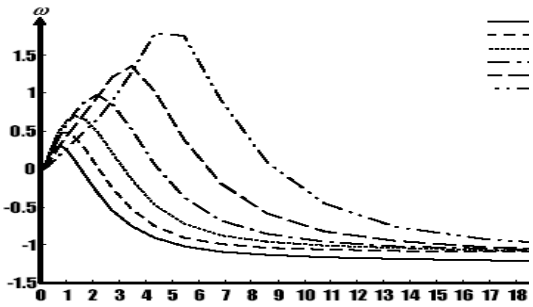

Fig. (17) Lower wall vorticity distribution downstream of back step for different values of Re at r=4:3

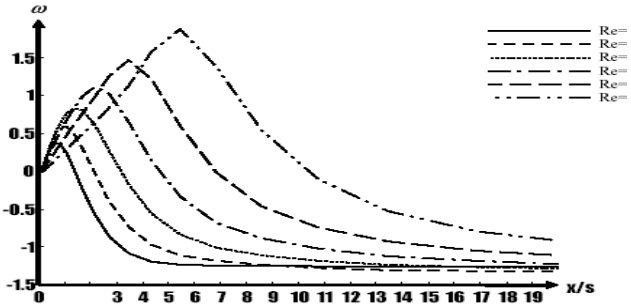

Fig. (18) Lower wall vorticity distribution downstream of back step for different values of Re at r=3:2

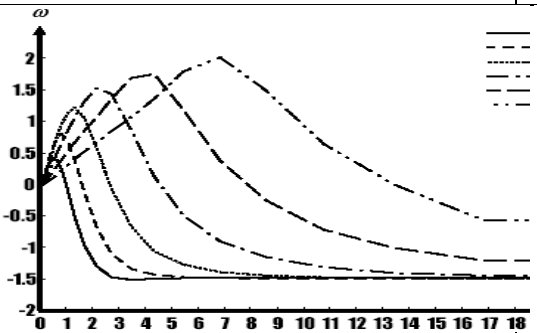

Fig. (19) Lower wall vorticity distribution downstream of back step for different values of Re at r=2:1

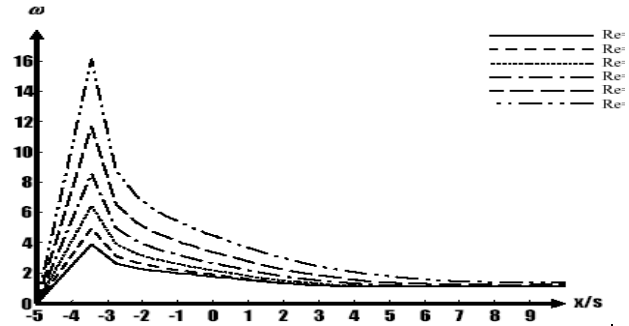

Fig. (20) Upper wall vorticity distribution downstream of back step for different values of Re at r=4:3

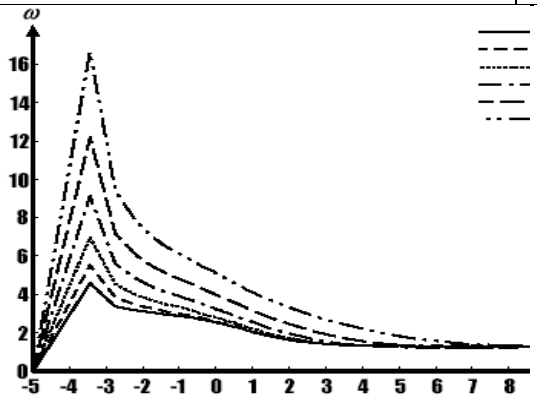

Fig. (21) Upper wall vorticity distribution downstream of back step for different values of Re at r=3:2

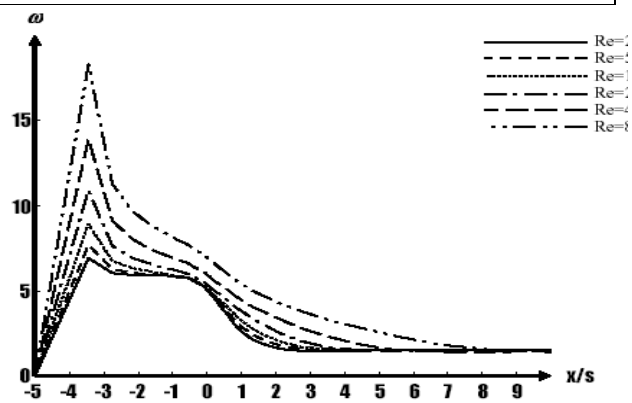

Fig. (22) Upper wall vorticity distribution downstream of back step for different values of Re at r=2:1

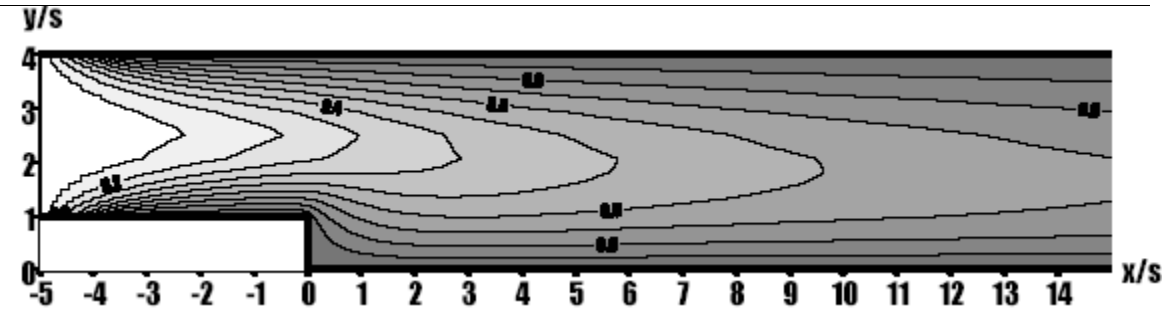

[a]: Re=25

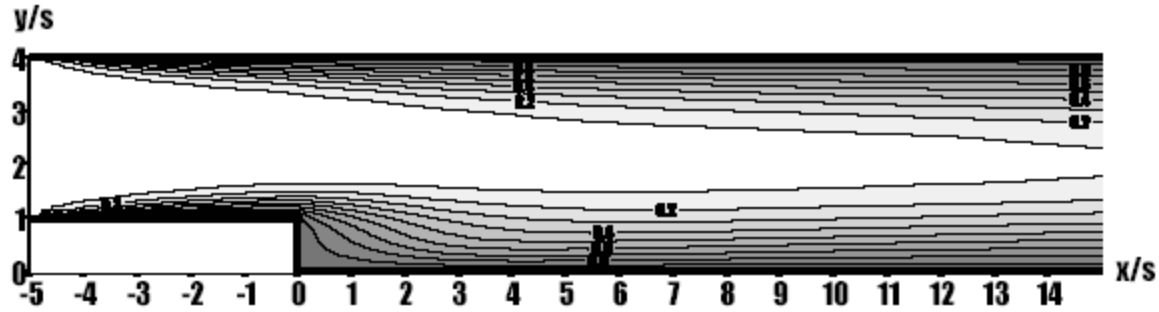

[b]: Re=200

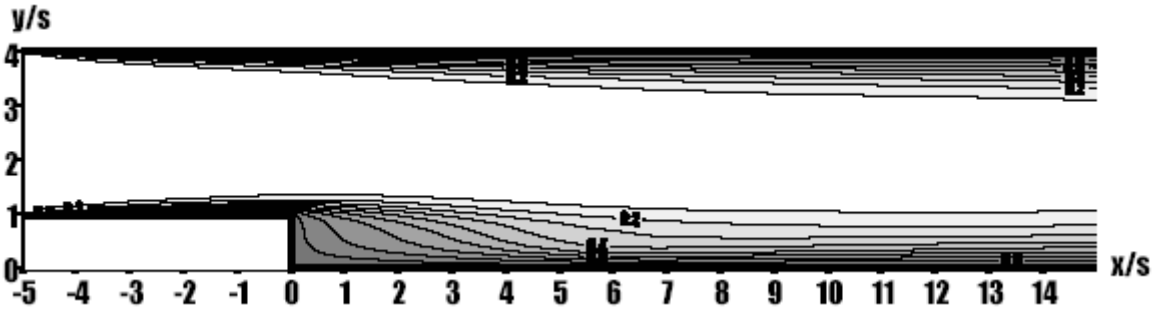

[c]: Re=800

Fig. (23) Isothermal contours for different of Reynolds number at r=4:3

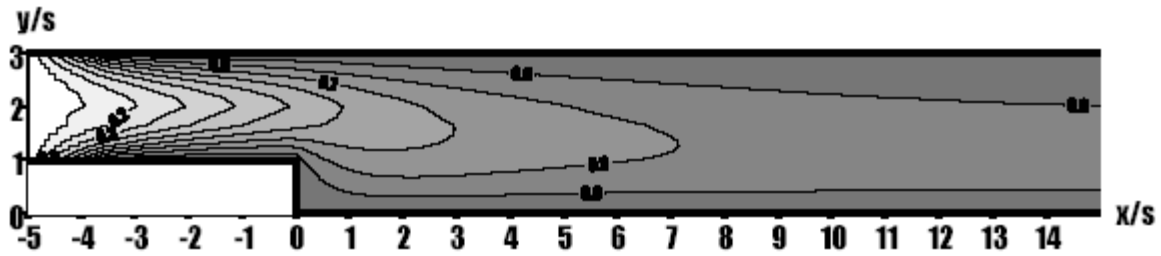

[a]: Re=25

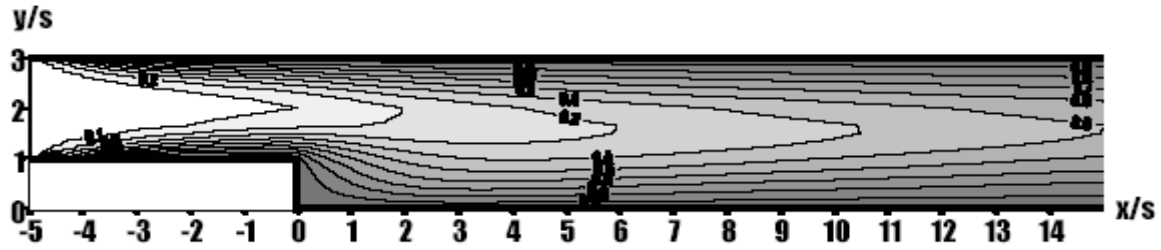

[b]: Re=200

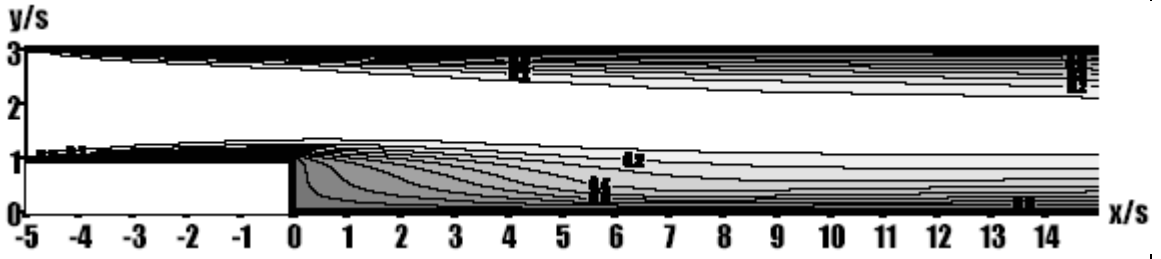

[c]: Re=800

Fig. (24) Isothermal contours for different of Reynolds number at r=3:2

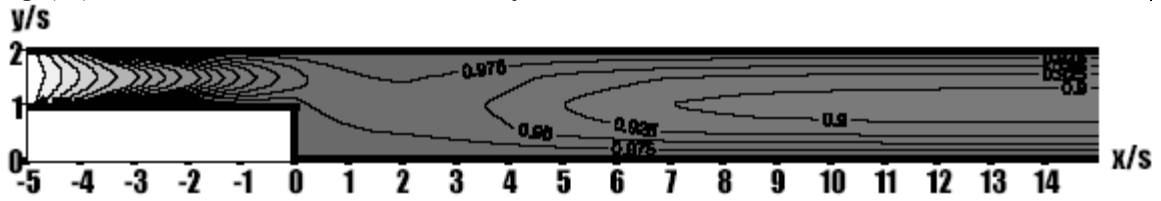

[a]: Re=25

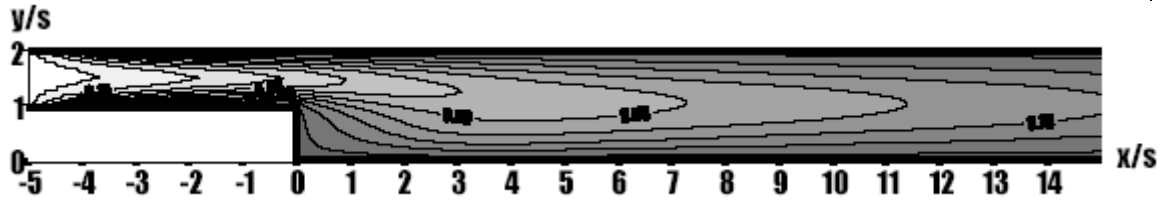

[b]: Re=200

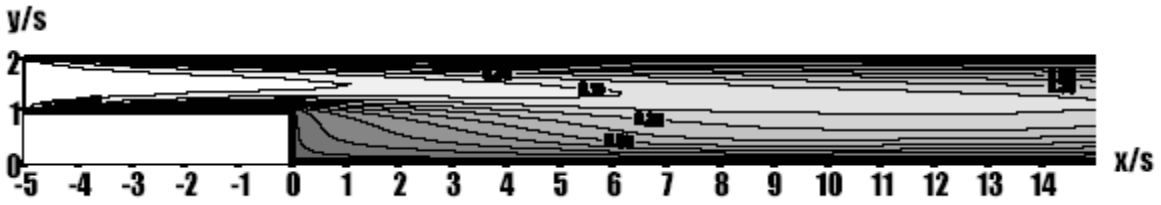

[c]: Re=800

Fig. (25) Isothermal contours for different of Reynolds number at r=2:1

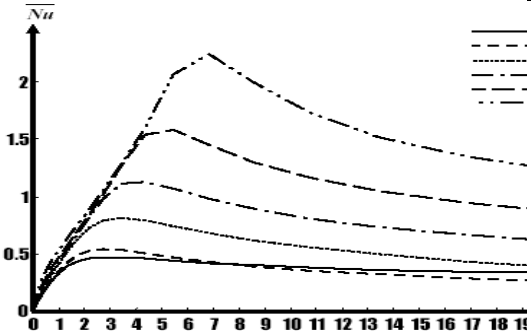

Fig. (26) Nuselt number distribution downstream of back step for different values of Re at r=4:3

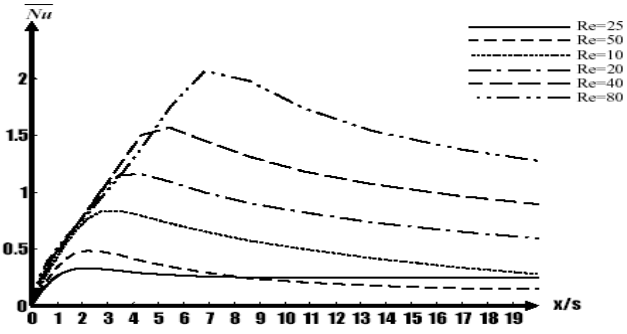

Fig. (27) Nuselt number distribution downstream of back step for different values of Re at r=3:2

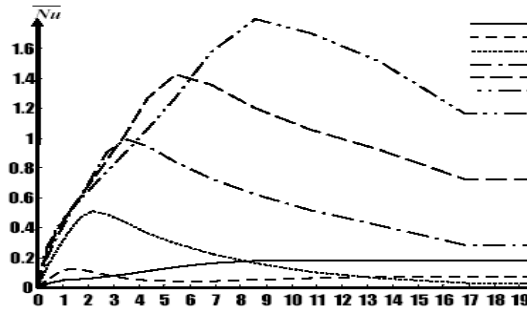

Fig. (28) Nuselt number distribution downstream of back step
for different values of Re at r=2:1

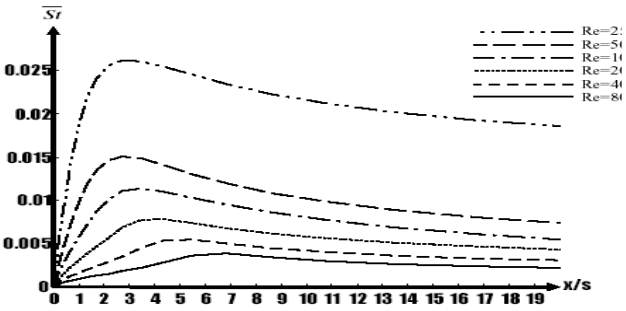

Fig. (29) Stanton number distribution downstream of back step for different values of Re at r=4:3 and P_r=0.72

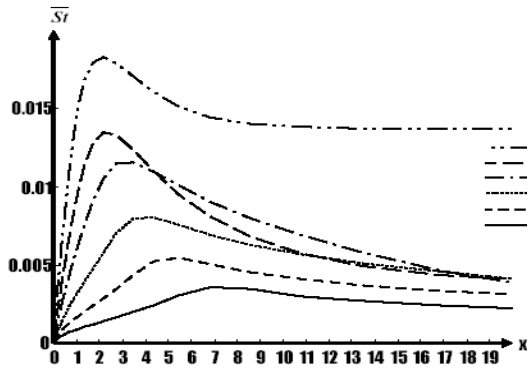

Fig. (30) Stanton number distribution downstream of back step for different values of Re at r=3:2 and P_r=0.72

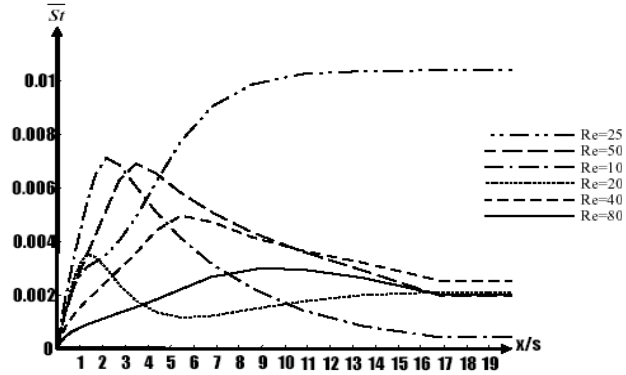

Fig. (31) Stanton number distribution downstream of back step for different values of Re at r=2:1 and P_r=0.72

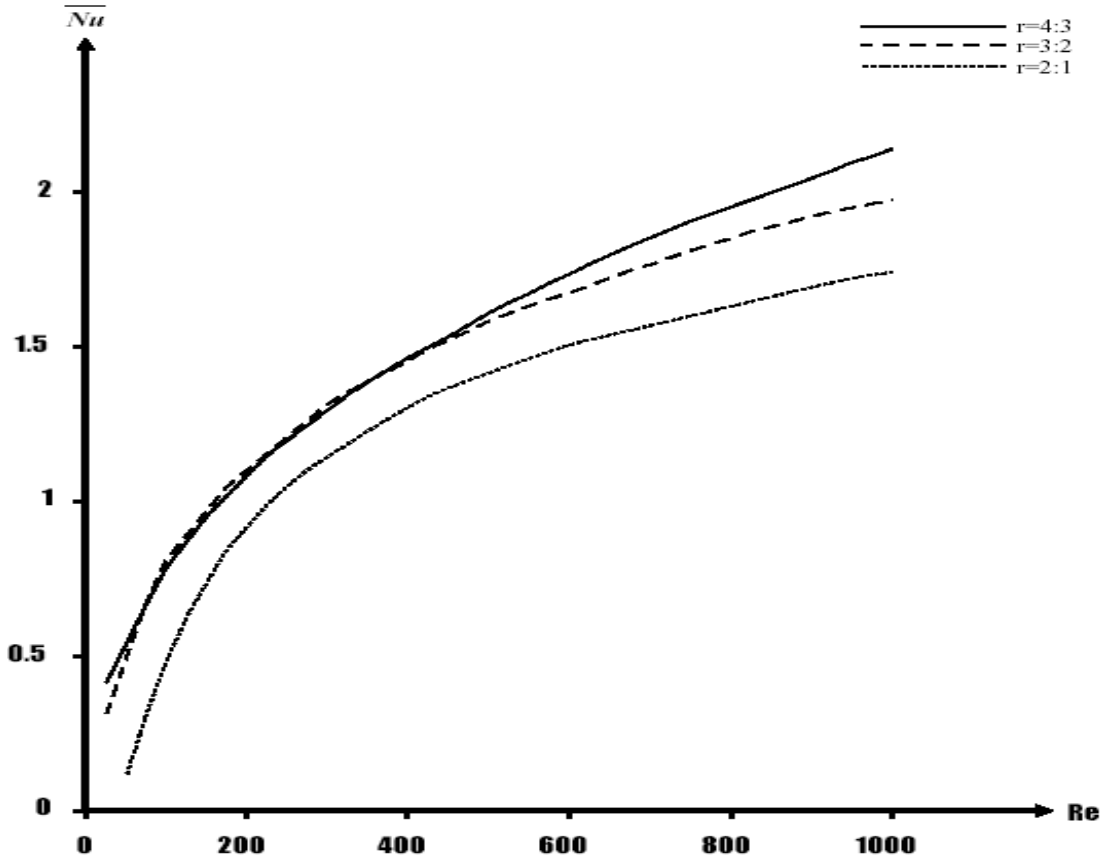

Fig.(32) Average Nuselt number vs. Renolds number for different of expansion ratios

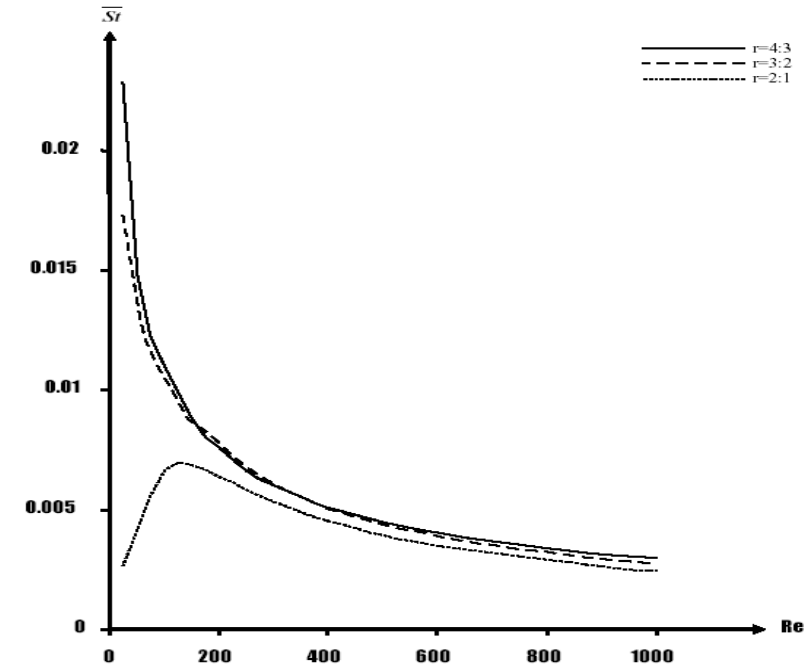

Fig.(33) Average Stanton number vs. Renolds number for different of expansion ratios and P_r=0072